Tissue-Engineered Soft-Tissue Reconstruction Using Noninvasive Mechanical Preconditioning and a Shelf-Ready Allograft Adipose Matrix

Giorgio Giatsidis, M.D., Ph.D.
Julien Succar, M.D.
Trevon D. Waters, B.S.
Wenyue Liu, M.D.
Patrick Rhodius, M.D.
Chenglong Wang, M.D.
Todd J. Nilsen, B.S.M.E.
Evangelia Chnari, Ph.D.
Dennis P. Orgill, M.D., Ph.D.

Boston, Mass.; Padova, Italy; Albuquerque, N.M.; Beijing, People's Republic of China; and Edison, N.J.

Background: Adipose tissue defects leading to severe functional (disability) and morphologic (disfigurement) morbidity are often treated in plastic surgery with fat grafting, which can be limited by resorption, necrosis, and cyst formation. This study aimed to assess whether adipose scaffolds could provide an environment for in situ autologous fat grafting, and to study whether adipose cell migration and proliferation (adipogenesis) within scaffolds could be enhanced by preliminarily increasing the vascularity (preconditioning) of the surrounding tissue receiving the scaffolds.

Methods: Using an established rodent model of subcutaneous tissue/scaffold grafting, the authors tested the potential of a human-derived, shelf-ready, injectable, decellularized allograft adipose matrix to reconstruct soft-tissue defects when used in combination with noninvasive mechanical (suction-induced) skin preconditioning.

Results: Combined use of the allograft adipose matrix and noninvasive skin preconditioning significantly improved long-term volume retention (50 to 80 percent higher at a 12-week follow-up) and histologic quality of reconstructed tissues compared with standard of care (autologous adipose grafts). The components of the allograft adipose matrix supported adipogenesis and angiogenesis. Combining the allograft adipose matrix with living adipose grafts mitigated negative outcomes (lower long-term volume retention, higher presence of cystic-like areas).

Conclusions: This study suggests that the synergistic use of the allograft adipose matrix and noninvasive tissue preconditioning provides an effective solution for improving fat grafting. These strategies can easily be tested in clinical trials and could establish the basis for a novel therapeutic paradigm in reconstructive surgery. (*Plast. Reconstr. Surg.* 144: 884, 2019.)

Adipose tissue loss is commonly associated with traumatic injuries, surgery, chronic disease, aging, or malformations.[1–4] Smaller defects can be restored by grafting adipose tissue. Grafted tissue initially survives on diffusion from recipient capillaries. When the metabolic demands of the grafted fat exceed the nutrient supply by diffusion, cells contained in the inner portion of the graft undergo ischemic necrosis, with subsequent formation of oil cysts.[5–8] For larger defects, surgeons often use conventional options, such as flaps or implant-based reconstructive procedures.[3,9–11]

Certain acellular scaffolds promote soft-tissue regeneration and avoid the ischemic necrosis observed in grafts of living tissues.[2,12–22] In particular, adipose scaffolds obtained through decellularization retain the native structural and biochemical characteristics that make them robust supporters of adipogenesis.[2,12–22] We previously investigated a novel allograft adipose matrix, derived from human cadaveric donor tissue, and observed that the allograft adipose matrix retains

From the Tissue Engineering and Wound Healing Laboratory, Division of Plastic Surgery, Department of Surgery, Brigham and Women's Hospital, Harvard Medical School; Department of Molecular Medicine, University of Padova; Preventive Medicine, University of New Mexico; Plastic Surgery Hospital, Chinese Academy of Medical Sciences and Peking Union Medical College; and the Musculoskeletal Transplant Foundation.

Received for publication August 31, 2018; accepted February 25, 2019.

DOI: 10.1097/PRS.0000000000006085

Related digital media are available in the full-text version of the article on www.PRSJournal.com.

its volume after in vivo grafting and also supports angiogenesis in recipient tissues.[23]

Here, we evaluate in a preclinical model the reconstructive potential of the allograft adipose matrix in comparison with the current fat grafting methods. We hypothesize that the allograft adipose matrix can provide an inductive microenvironment for adipose tissue migration and proliferation. We further investigate the combination of the allograft adipose matrix and noninvasive, suction-based recipient-site preconditioning (i.e., external volume expansion).[24–29] Preclinical studies have demonstrated that controlled application of suction to soft tissues induces a subcritical tissue ischemia, triggering a proangiogenic response: the net result is a robust increase in the vascular density of treated tissue. As previous research has shown that external volume expansion improves the survival of tissue grafts by creating a more well-vascularized and proadipogenic recipient site,[30,31] we postulate that combination with external volume expansion might synergistically improve the outcomes of the allograft adipose matrix.

MATERIALS AND METHODS

Animals and Study Design

This study was carried out with respect for high ethical standards. All the studies have been approved, when required, by the appropriate ethics committee and have therefore been performed in accordance with and in conformity to the World Medical Association Declaration of Helsinki (June of 1964) and subsequent amendments. All animal experiments have been designed and performed in accordance with the Animal Research: Reporting of In Vivo Experiments guidelines and the National Institutes of Health *Guide for the Care and Use of Laboratory Animals* (National Institutes of Health publication no. 8023, revised 1978). The study involved 54 female, 10-week old, athymic mice (NU/J) (strain 002019; Jackson Laboratories, Bar Harbor, Me.). This mouse strain tolerates xenografts without rejection. The study compared six groups: external volume expansion only; adipose tissue graft only (fat); allograft adipose matrix graft only; combined allograft adipose matrix and adipose tissue grafts (allograft adipose matrix plus fat); external volume expansion and allograft adipose matrix graft (external volume expansion plus allograft adipose matrix); and combined external volume expansion, allograft adipose matrix, and adipose tissue grafts (external volume expansion plus allograft adipose matrix plus fat). For each animal, both sides of the dorsum were randomly allocated to a treatment group, resulting in a total number of samples/recipient sites to 108 (54 × 2). After surgery, animals were followed up for 4 weeks (n = 4 per group) and 12 weeks (n = 16 per group, except for the external volume expansion–only group, which was n = 4 because this group received no graft and was mostly used as a negative control) before collecting samples of the grafts (skin only in the external volume expansion group) for analysis.

Disclosure: *Dr. Orgill is a consultant for the Musculoskeletal Transplant Foundation (MTF) and KCI, Inc., and receives research funding through a sponsored research agreement from MTF and KCI to Brigham and Women's Hospital. Mr. Nilsen and Dr. Chnari are employees of MTF. All other authors declare no actual or potential conflict of interests. They report no commercial or financial associations, personal or other relationships with other people or organizations that could inappropriately influence the reported artilce or create a conflict of interest with the information presented. Dr. Giatsidis and Dr. Orgill have filed a patent based on methods described in this article (PCT/US2016/018164: "Methods and Apparatus for Promotion of Angiogenesis and Adipogenesis in Tissues Through the Application of Mechanical Forces") and hold rights as inventors in accordance to their institutional policies. MTF employees were involved in study design, tissue preparation, description of the process in the Methods and review of the final draft for flow and accuracy. They did not influence the reporting of the results or the final conclusions of the article.*

External Volume Expansion Model

We adopted our previously described model of external volume expansion[24,27,30] (Fig. 1). A 1-cm^3 silicone cup was applied to the dorsum of animals (1 cm lateral to the spine) and connected to a vacuum pump. Suction at 25 mmHg was delivered six times/day (30 minutes sessions with 1-hour breaks in-between).[30] Animals received external volume expansion treatment from day 10 to day 5 before surgery (total treatment duration, 5 days).

Subcutaneous Injection Model

A 0.3-cc aliquot was injected on the lateral dorsum of animals through a distal surgical access using a 16-gauge cannula (Blunt Injector; Marina Medical Instruments, Inc., Sunrise, Fla.) over a

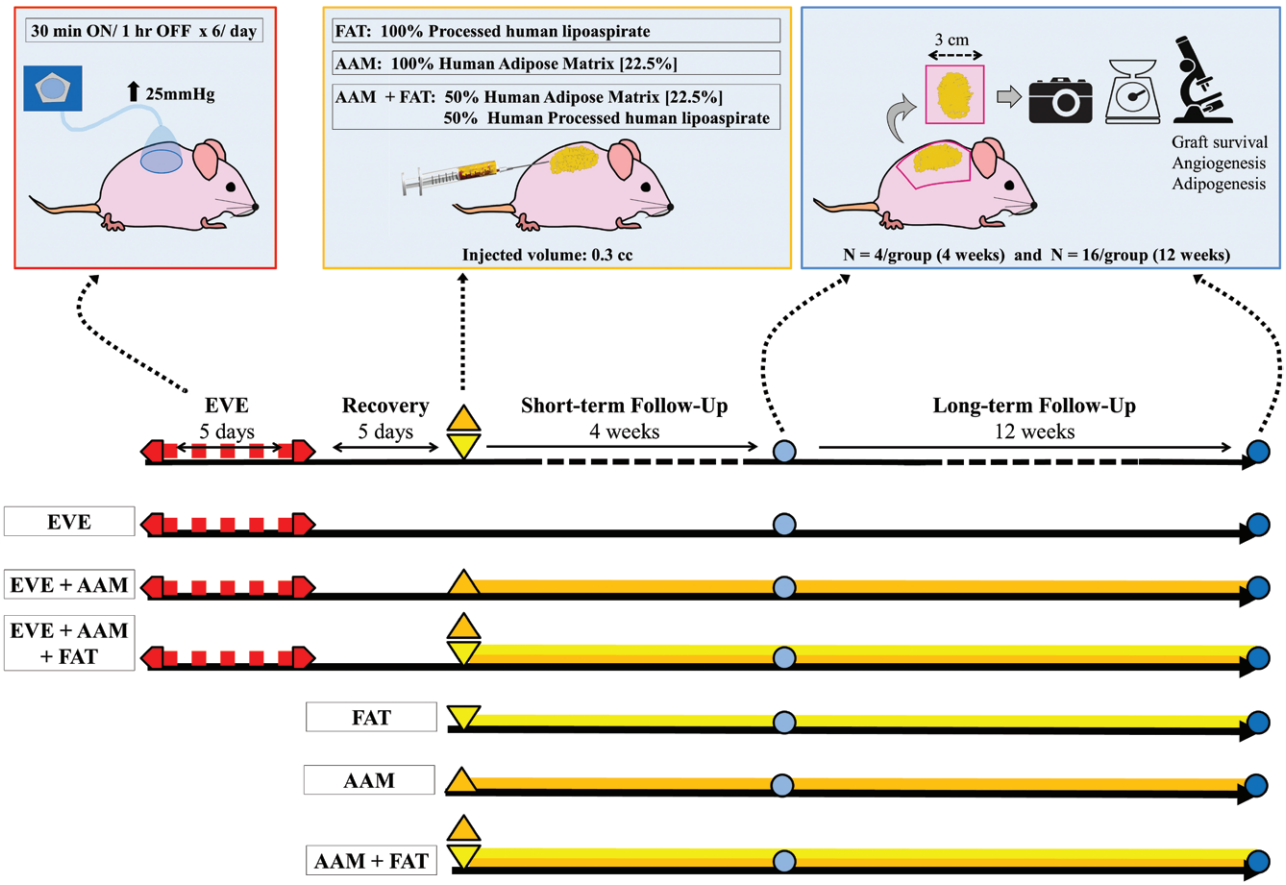

Fig. 1. Experimental study design and procedures. (*Above*, *left*) Representation of tissue preconditioning with external volume expansion (*EVE*) using moderate-intensity intermittent kinetics (30 minutes on/1 hour off, 6 times per day for 5 days) and a 25-mmHg suction provided by a pump and delivered through a dome-shaped silicone interface. (*Above*, *center*) Representation of the preparation of the different grafts and of the grafting technique in the subcutaneous lateral dorsum of animals. *FAT*, adipose tissue; *AAM*, allograft adipose matrix; *ECM*, extracellular matrix. (*Above*, *right*) Representation of the analytic techniques adopted to assess outcomes and the number of samples analyzed at each time point. *Camera*, digital imaging; *balance*, specimen weight; *microscope*, microscopic analysis through histology. (*Center*) Study design. *Red dotted line*, external volume expansion; *orange triangles and lines*, allograft adipose matrix graft; *yellow triangles and lines*, adipose tissue graft; *blue dots*, time points for digital imaging and tissue procurement.

length of 3 cm (Fig. 1). [**See Video (online)**, which shows the technique adopted for subcutaneous placement of tissue grafts in the lateral dorsum of animals, using a tunnel technique and a caudal approach in proximity of the root of the tail.] The choice of the volume was based on previous optimization studies.

Adipose Tissue Graft Preparation

Lipoaspirate (approximately 50 cc/session) was obtained by manual liposuction (12 G Micro-Khouri Harvester; Marina Medical Instruments) from discarded human panniculectomies and processed in a sterile fashion.[32] The lipoaspirate was centrifuged at approximately 1800 *g* for 3 minutes to separate the adipose tissue from the oil part and the stromal vascular fraction: both components were discarded to obtain the processed adipose tissue (fat). [**See Figure, Supplemental Digital Content 1**, which shows (*left*) preparation of processed adipose tissue grafts from human lipoaspirate through centrifugation. (*Right*) Appearance of the processed adipose tissue grafts, the rehydrated allograft adipose matrix, and the combination of the two in 1-ml syringes before injection. *SVF*, stromal vascular fraction; *AAM*, allograft adipose matrix, ***http://links.lww.com/PRS/D689***.] Human tissues were procured under a protocol approved by our institutional review board. Tissue from two donors was used in this study (Table 1). Animals were divided in two rounds of experiments (4- and 12-week follow-up): in each round, animals

Table 1. Clinical Characteristics of Donor Patients for Adipose Tissue

Donor	Age (yr)	Sex	Weight (lb)	Height	BMI (kg/m^2)	Donor Site	History of Diabetes	Smoking Habit
1	53	Female	234	5′5″	38.9	Abdominal wall (superficial adipose layer)	No	Yes (former)
2	50	Female	192	5′9″	28.3	Abdominal wall (superficial adipose layer)	No	Yes (former)

BMI, body mass index.

received adipose grafts from the same donor and the lipoaspirate was used within 1 hour after procurement. In round 1 (4-week follow-up), six animals (12 recipient sites) received adipose grafts (n = 4 sites per group for the groups adipose tissue, allograft adipose matrix plus adipose tissue, and external volume expansion plus allograft adipose matrix plus adipose tissue). In round 2 (12-week follow-up), 24 animals (48 recipient sites) received adipose grafts (n = 16 sites per group for groups adipose tissue, allograft adipose matrix plus adipose tissue, and external volume expansion plus allograft adipose matrix plus adipose tissue).

Allograft Adipose Matrix Preparation

Allograft adipose matrix was provided by the Musculoskeletal Transplant Foundation (Edison, N.J.) and obtained from processed human adipose tissue of cadaveric donors.[23] Human donor cells are removed from the allograft adipose matrix to minimize an immune reaction to cells. The allograft adipose matrix has passed International Organization for Standardization 10993 biocompatibility tests, and has successfully been used clinically.[33]

The allograft adipose matrix was provided in a lyophilized and sterilized injectable powder containing small particles (approximately 100 to 200 μm^2). The allograft adipose matrix was reconstituted with sterile saline solution to obtain a 23 percent rehydration ratio (protein mass–to–saline volume ratio) before in vivo injection. This ratio was determined by our previous optimization studies.[23]

Allograft Adipose Matrix plus Adipose Tissue Graft Preparation

The rehydrated allograft adipose matrix was mixed in equal parts (50 percent ratio, based on mass weight) with processed lipoaspirate using two Luer-lock syringes and a connector (Fig. 1) (**see Figure, Supplemental Digital Content 1**, ***http://links.lww.com/PRS/D689***). This ratio was determined by our previous optimization studies.[23]

Macroscopic and Microscopic Analysis

Study samples were procured en bloc by precisely cutting 2 × 2-cm sections of the integument (including the graft, the overlaying/surrounding skin, and the panniculus carnosus) (Fig. 1). Fresh samples were weighed with a precision scale (OHAUS Corp., Parsippany, N.J.).

All samples were fixed in 10% neutral-buffered formaldehyde and stored in 70% ethanol at 4°C. Hematoxylin and eosin staining was used to measure graft thickness and the cross-sectional area of the graft. The cross-sectional area of the graft was used as a surrogate for graft volume, assuming a homogeneous behavior of the graft in all its components. The Aperio System (Leica Biosystems, Wetzlar, Germany) was used for slide scanning, and ImageJ software (National Institutes of Health, Bethesda, Md.) was used for image analysis.

Immunohistochemistry was used to quantify graft and perigraft angiogenesis, through the endothelial cell marker platelet endothelial cell adhesion molecule-1 (CD31, 1:100; catalogue no. ab28364; Abcam, Cambridge, Mass.), and graft inflammation, through a pan-leukocyte marker (CD45, 1:100; catalogue no. ab10558; Abcam). Images of the microscopy slides were acquired at a standard magnification (40×) using a Nikon E200 microscope (Nikon Corp., Tokyo, Japan) and quantified using ImageJ software. Image acquisition and analysis were performed according to established methods.[27,30] Three images in 40× fields were obtained randomly from areas of the sample. Vascular density was quantified as the number of CD31$^+$ vessels identified in each of the 40× fields. Immunofluorescence was used to qualitatively analyze adipocyte proliferation/infiltration within the graft, using the lipid droplet surface marker perilipin.

Data and Statistical Analysis

The sample size was calculated to detect meaningful differences (alpha = 0.05; power = 95 percent) between treated groups and controls with regard to the primary endpoint (graft

cross-sectional area at 12-week follow-up, measured with histology; expected difference, 30 to 35 percent). Six-week data were used for qualitative analysis with no statistical analysis performed, given the small size of groups. These data were represented as mean ± SD and using bar graphs to allow a more direct comparison to data from the longer-term follow-up. Data were analyzed by three researchers, blinded to the groups. Differences between groups were expressed as the mean ± SD. The significance of differences ($p < 0.05$) was evaluated with one-way analysis of variance and Bonferroni post hoc correction (GraphPad Prism v7; GraphPad Software, Inc., San Diego, Calif.).

RESULTS

Combining External Volume Expansion and Allograft Adipose Matrix Grafting Maximizes Volume Retention and Soft-Tissue Reconstruction

At the 12-week follow-up, the group that had received a combined treatment using recipient-site preconditioning with external volume expansion and subsequent allograft adipose matrix grafting (external volume expansion plus allograft adipose matrix) showed a significantly higher graft volume retention in comparison to all other groups except the allograft adipose matrix group, as measured through histologic evaluation, specimen weight (standardized graft plus surrounding tissue biopsy specimen), and macroscopic observation of the dissected tissue. In the external volume expansion plus allograft adipose matrix group, the cross-sectional area of the grafts at the 12-week follow-up was 82 percent higher than in the control (adipose tissue graft) group (6.2 ± 2.8 mm^2 versus 3.4 ± 2.8 mm^2; $p < 0.05$) (Fig. 2 and Table 2). [**See Figure, Supplemental Digital Content 2**, which shows measurement of survival (volume) of grafts. Histologic appearance (whole-graft scanning of hematoxylin and eosin–stained slides) of grafts at short-term (4 weeks) and long-term (12 weeks) follow-up, showing volume retention of grafts (measured as cross-sectional area at histologic sections) as a method to assess their survival (original magnification, × 22; *scale bar* = 1400 μm), ***http://links.lww.com/PRS/D690***.] When compared to other combined treatments (combined adipose tissue and allograft adipose matrix graft, and combined preconditioning with external volume expansion and subsequent adipose tissue–allograft adipose matrix graft), the external volume expansion plus allograft adipose matrix group also showed a significantly better outcome. The cross-sectional area was 56 percent higher than in the allograft adipose matrix plus adipose tissue group (4.0 ± 0.8 mm^2; $p < 0.05$) and 87 percent higher than in the external volume expansion plus allograft adipose matrix plus adipose tissue group (3.3 ± 1.8 mm^2; $p < 0.05$) (Fig. 2 and Table 2) (**see Figure, Supplemental Digital Content 2**, ***http://links.lww.com/PRS/D690***). The allograft adipose matrix group showed a significantly higher cross-sectional area compared with the external volume expansion plus allograft adipose matrix plus adipose tissue group, but not when compared to the adipose tissue control group. No differences were observed between groups at an earlier time point

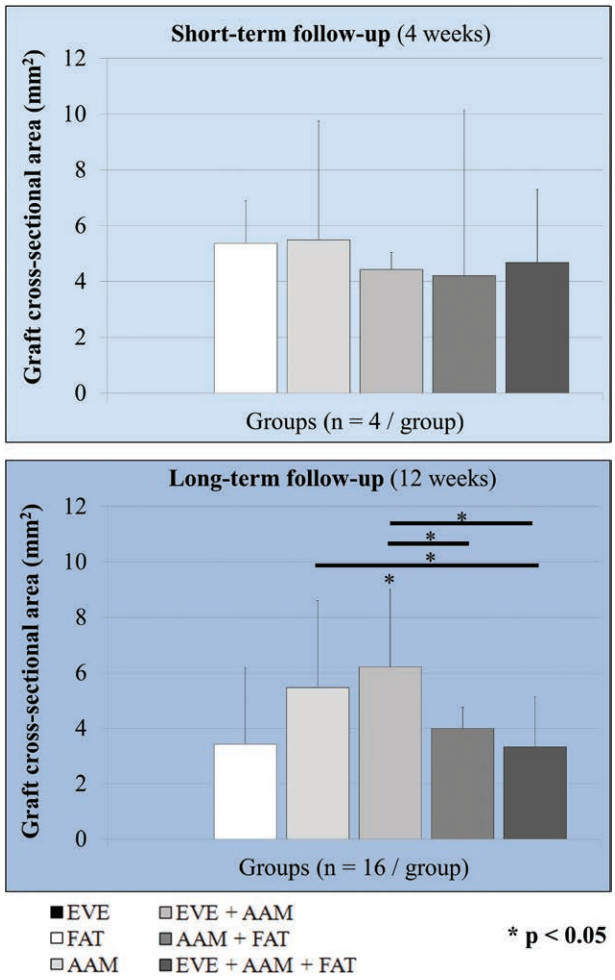

Fig. 2. Measurement of survival (volume) of grafts. Cross-sectional area of grafts measured with histology on microscopic samples. One-way analysis of variance with Bonferroni post hoc correction. A value of $p < 0.05$ was considered statistically significant. Data are expressed as mean ± SD. *EVE*, external volume expansion; *FAT*, adipose tissue; *AAM*, allograft adipose matrix.

Table 2. Data for All Measurements*

Parameter	Short-Term Follow-Up (4 Wk)	Long-Term Follow-Up (12 Wk)
Graft weight, g		
EVE	0.3 ± 0	0.4 ± 0.1
Fat	0.4 ± 0.1	0.5 ± 0.1
AAM	0.5 ± 0.1	0.6 ± 0.1
EVE plus AAM	0.6 ± 0.1	0.7 ± 0.1
AAM plus fat	0.6 ± 0.1	0.6 ± 0.1
EVE plus AAM plus fat	0.6 ± 0.1	0.6 ± 0.1
Graft cross-sectional area, mm^2		
EVE	n/a	n/a
Fat	5.4 ± 1.5	3.4 ± 2.8
AAM	5.5 ± 4.3	5.5 ± 3.1
EVE plus AAM	4.4 ± 0.6	6.2 ± 2.8
AAM plus fat	4.2 ± 5.9	4.0 ± 0.8
EVE plus AAM plus fat	4.7 ± 2.6	3.3 ± 1.8
Graft angiogenesis (blood vessels per 40× magnification field)		
EVE	n/a	n/a
Fat	33 ± 4	43.8 ± 11.9
AAM	39.3 ± 6	79.7 ± 24.9
EVE plus AAM	47 ± 6	69.2 ± 21.0
AAM plus fat	24 ± 13	83.3 ± 27.0
EVE plus AAM plus fat	41 ± 33	84.8 ± 30.4
Perigraft angiogenesis (blood vessels per 40× magnification field)		
EVE	58 ± 15	62.8 ± 27.2
Fat	52 ± 9	60.3 ± 18.3
AAM	42 ± 15	59.4 ± 24.2
EVE plus AAM	46 ± 6	54.8 ± 24.2
AAM plus fat	59 ± 13	70.5 ± 20.6
EVE plus AAM plus fat	45 ± 9	68.5 ± 20.1

n/a, not applicable; EVE, external volume expansion; FAT, adipose tissue; AAM, allograft adipose matrix.
*Data are expressed as mean ± SD.

(short-term follow-up, 4 weeks). Gradual graft reabsorption (58 percent loss) could be observed in the adipose tissue group when comparing values at earlier (short-term follow-up, 4 weeks) and later (long-term follow-up, 12 weeks) time points; instead, both the allograft adipose matrix and the allograft adipose matrix plus adipose tissue group grossly retained the same values over time. Weights of the samples at 12 weeks are reported in supplemental materials (Table 2). [**See Figure, Supplemental Digital Content 3**, which shows graft survival at follow-up. Statistical analysis was performed using one-way analysis of variance with Bonferroni post hoc correction. A value of $p < 0.05$ was considered statistically significant. Data are expressed as the mean ± SD. Weight of graft specimens after procurement at short-term (4 weeks) and long-term (12 weeks) follow-up. *EVE*, external volume expansion; *FAT*, adipose tissue; *AAM*, allograft adipose matrix, ***http://links.lww.com/PRS/D691***. **See Figure, Supplemental Digital Content 4**, which shows macroscopic appearance of grafts at follow-up. Digital imaging of the external macroscopic appearance of the grafts (each row represents a different animal) immediately after surgery, at short-term (4 weeks) follow-up, and at long-term follow-up (12 weeks) showing differing volume retention between groups. (*Right*) Internal (dissected) macroscopic appearance of grafts after procurement at 12-week follow-up, confirming observations drawn from the external macroscopic appearance (*scale bar* = 1 cm for both). *EVE*, external volume expansion; *FAT*, adipose tissue; *AAM*, allograft adipose matrix, ***http://links.lww.com/PRS/D692***.]

Allograft Adipose Matrix Supports Adipogenesis without the Formation of Cystic Necrotic Areas

In both the allograft adipose matrix and the external volume expansion plus allograft adipose matrix groups, gradual migration and proliferation of adipocyte-like cells was evident along the margins of grafts at short-term (4 weeks) follow-up; the core of the graft demonstrated presence of the endogenous extracellular matrix components of the allograft adipose matrix with a lack of cells. [**See Figure, Supplemental Digital Content 5**, which shows measurement of survival (quality) of grafts and adipogenesis. Histologic appearance (whole-graft scanning of hematoxylin and eosin–stained slides) of grafts at short-term (4-week) and long-term (12-week) follow-up, showing the architecture of grafts, the presence of infiltrating/proliferating cells, and the presence of cystic areas as a method of assessing adipogenesis and survival of grafts (original magnification, × 3). *Scale bars* = 450 μm; *H&E*, hematoxylin and eosin; *EVE*, external volume expansion; *FAT*, adipose tissue; *AAM*, allograft adipose matrix; *triangles*, $CD31^+$ blood vessel; *right arrow*, adipocytes; *stars*, cystic areas; *right arrowheads*, allograft adipose matrix, ***http://links.lww.com/PRS/D693***.] At a longer follow-up (12 weeks), adipocyte-like cells appeared to have replaced most of the extracellular matrix core of the allograft adipose matrix graft. In the external volume expansion plus allograft adipose matrix group, the clusters of migrating and proliferating adipocytes appeared higher in number compared with the allograft adipose matrix group at both time points. Immunohistochemical analysis using the perilipin marker confirmed the adipocytic nature of these cells (Fig. 3).

In groups containing adipose tissue grafts, the presence of living cells was observed along with the presence of multiple cystic areas. Cystic areas, representative of necrotic phenomena, were greater in number and size in the adipose tissue group and slightly less frequent in the allograft adipose

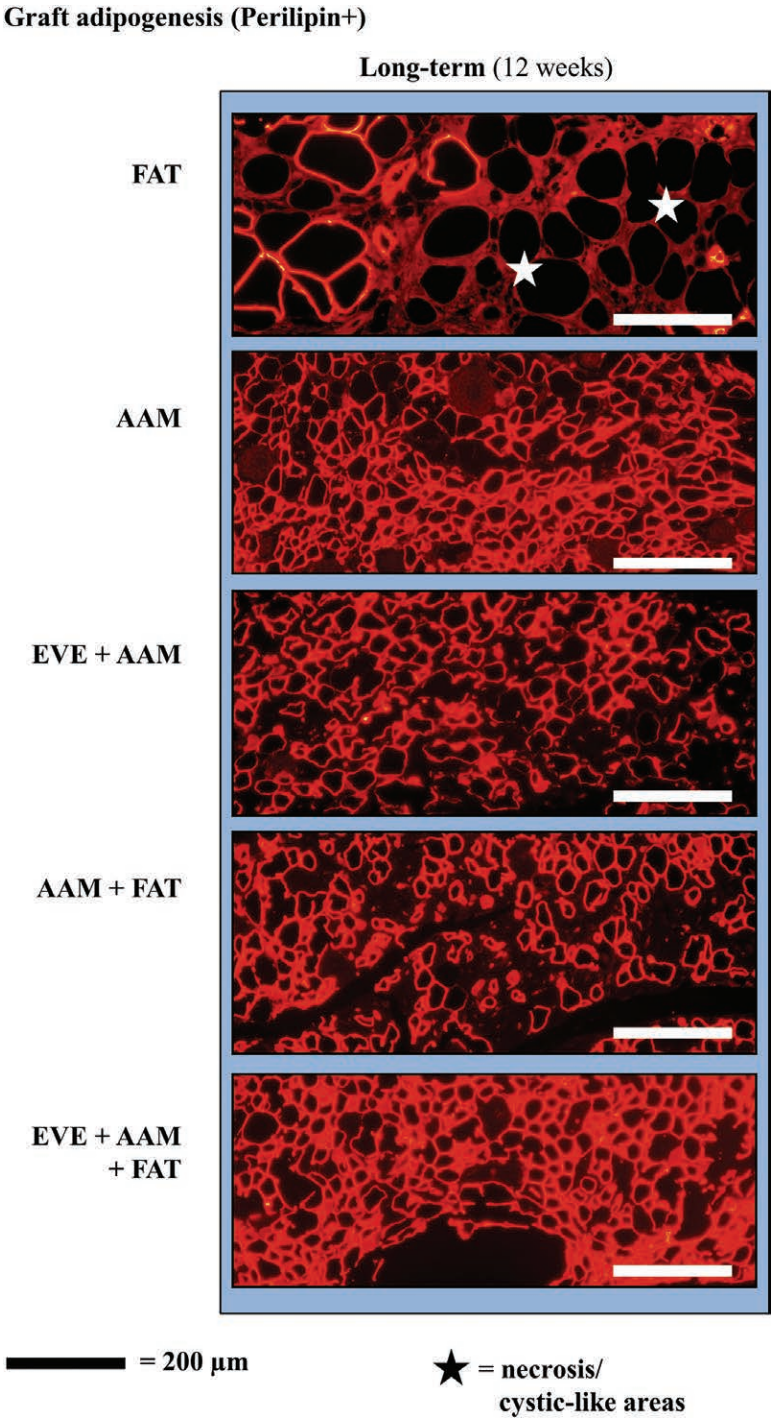

Fig. 3. Graft survival and adipogenesis within the grafts. Histologic staining (perilipin, immunofluorescence) of the grafts showing different presence of living adipocytes (red staining: cell membrane of adipocytes) and necrotic vacuoles or cystic areas (unstained areas) (original magnification, × 40). *Scale bars* = 200 µm. *EVE*, external volume expansion; *FAT*, adipose tissue; *AAM*, allograft adipose matrix; *stars*, necrosis/cystic areas.

matrix plus adipose tissue and the external volume expansion plus allograft adipose matrix plus adipose tissue groups. Histologic evaluation of the two latter groups presented features of both the allograft adipose matrix or external volume expansion plus allograft adipose matrix grafts

(extracellular matrix core, marginal adipogenesis) and the adipose tissue grafts (interspersed adipose cells, presence of cystic areas) (**see Figure, Supplemental Digital Content 5**, ***http://links.lww.com/PRS/D693***). Immunofluorescence (perilipin) further confirmed these outcomes and the presence of necrotic cystic areas in adipose tissue grafts (denser) and in the allograft adipose matrix plus adipose tissue and the external volume expansion plus allograft adipose matrix plus adipose tissue groups (less diffused) (Fig. 3).

In all groups containing the allograft adipose matrix, further immunohistochemical analysis (CD45, panleukocyte marker) showed the presence of numerous inflammatory cells close to the clusters of adipocytes infiltrating the graft. [**See Figure, Supplemental Digital Content 6**, which shows perigraft and graft inflammation. CD45 (panleukocyte marker) immunohistochemistry showing presence of inflammatory cells surrounding the clusters of proliferating adipocytes in the groups containing the allograft adipose matrix. In the adipose tissue group, inflammation surrounds cystic areas of necrosis (original magnification, × 40). *Scale bars* = 200 μm. *EVE*, external volume expansion; *FAT*, adipose tissue; *AAM*, allograft adipose matrix; *thin arrows*, adipocytes; *stars*, cystic areas; *thick arrows*, inflammatory cells, ***http://links.lww.com/PRS/D694***.] The presence of inflammation was reduced in the groups in which the allograft adipose matrix was combined with adipose tissue (allograft adipose matrix plus adipose tissue and external volume expansion plus allograft adipose matrix plus adipose tissue). Different from other samples, in the adipose tissue group, inflammatory cells aligned along the cystic areas of necrosis and did not cluster next to proliferating adipocytes.

Allograft Adipose Matrix Supports Graft Angiogenesis

No significant differences were observed in the density of blood vessels at 12-week follow-up. [**See Figure, Supplemental Digital Content 7**, which shows (*left*) angiogenic effect (variations in blood vessels density) in the skin surrounding the grafts. Statistical analysis was performed using one-way analysis of variance with Bonferroni post hoc correction. A value of $p < 0.05$ was considered statistically significant. Values are expressed as the mean ± SD. (*Right*) Data for histologic measurements. *EVE*, external volume expansion; *FAT*, adipose tissue; *AAM*, allograft adipose matrix, ***http://links.lww.com/PRS/D695***.] In addition, no differences were noted in groups that received preconditioning with external volume expansion and a subsequent graft (external volume expansion plus allograft adipose matrix or external volume expansion plus allograft adipose matrix plus adipose tissue) and those that did not receive a graft (external volume expansion only).

At 12 weeks, groups containing the allograft adipose matrix (with or without combined treatments) had a statistically significant higher density of blood vessels inside the grafts (82 to 93 percent higher, depending on groups) when compared to control adipose tissue grafts ($p < 0.05$ for all groups) (Fig. 4 and Table 2). [**See Figure, Supplemental Digital Content 8**, which shows graft blood vessel density and angiogenic effect of the allograft adipose matrix. CD31 (endothelial marker)

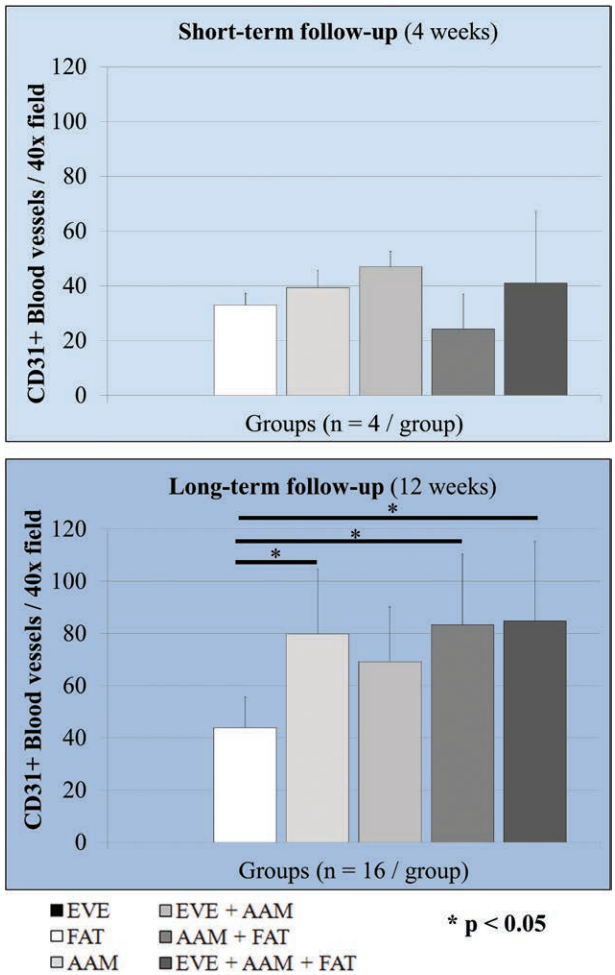

Fig. 4. Graft blood vessel density and angiogenic effect of the allograft adipose matrix. Outcomes of measurements of blood vessel density on histologic images. One-way analysis of variance with Bonferroni post hoc correction. A value of $p < 0.05$ was considered statistically significant. Data are expressed as mean ± SD. *EVE*, external volume expansion; *FAT*, adipose tissue; *AAM*, allograft adipose matrix.

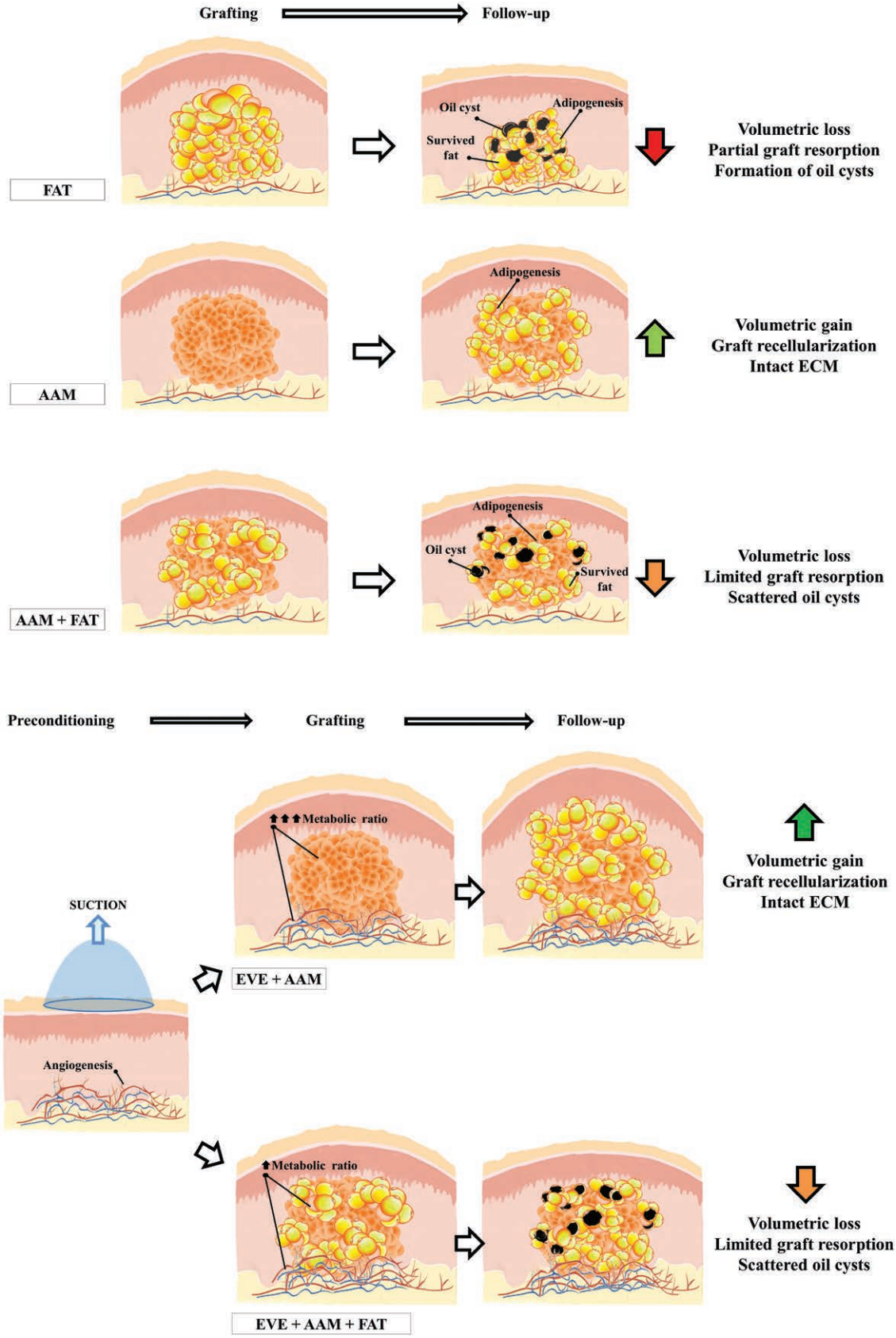

Fig. 5. Postulated mechanisms of action and conceptual representation of graft survival and soft-tissue regeneration achieved using different strategies that combine adipose tissue grafts (*FAT*), an acellular allograft adipose

immunohistochemistry of grafts at short-term (4 weeks) and long-term (12 weeks) follow-up, showing presence of blood vessels within the grafts and their morphology, as a method of assessing angiogenesis (original magnification, × 40). *Scale bars* = 250 μm. *EVE*, external volume expansion; *FAT*, adipose tissue; *AAM*, allograft adipose matrix; *right arrowheads*, $CD31^+$ blood vessels, ***http://links.lww.com/PRS/D696***.] The external volume expansion plus allograft adipose matrix group did not have a statistically significant increase in the density of blood vessels within the graft compared with the adipose tissue graft (respectively, 69 ± 21 vessels/40× magnification field versus 44 ± 12 vessels/40× magnification field; $p > 0.05$) (Fig. 4 and Table 2). No significant differences were observed between groups containing the allograft adipose matrix (allograft adipose matrix, allograft adipose matrix plus adipose tissue, external volume expansion plus allograft adipose matrix plus adipose tissue), even when compared to the external volume expansion plus allograft adipose matrix group. Within each group, only the allograft adipose matrix plus adipose tissue showed a statistically significant increase in graft vascularization from week 4 to week 12 ($p < 0.01$). When compared to native adipose tissue (inguinal fat pad), the latter demonstrated a significantly higher density of blood vessels (**see Figure, Supplemental Digital Content 8**, ***http://links.lww.com/PRS/D696***).

DISCUSSION

We show that a previously optimized allograft adipose matrix assists adipose tissue formation,[23] supporting migration and proliferation of adipocytes (adipogenesis) and endothelial vessels (angiogenesis). Allograft adipose matrix grafts retain their volume and restore a native adipose architecture (Fig. 5, *left*). Our studies show that when allograft adipose matrix grafts are combined with adipose tissue grafts, the negative outcomes associated with the adipose tissue grafts are partially mitigated (Fig. 5).

Fig. 5. ***(Continued)*** matrix (*AAM*), and noninvasive recipient-site preconditioning with external volume expansion (*EVE*). (*Left*) Strategies and outcomes associated with adipose tissue, allograft adipose matrix, or combined allograft adipose matrix plus adipose tissue grafts. *ECM*, extracellular matrix. (*Right*) Strategies and outcomes associated with allograft adipose matrix or allograft adipose matrix plus adipose tissue grafts combined with external volume expansion.

When allograft adipose matrix grafts are combined with external volume expansion, outcomes are further enhanced (82 percent higher volume at 12-week follow-up compared with control adipose grafts) (Fig. 5). External volume expansion induces adipogenesis in tissues[24] and creates a subcritical hypoxic environment, eliciting angiogenesis; possibly, vascular endothelial growth factor mediated. This effect increases the vascular density (approximately 2-fold) of target tissues.[27,30,34] Cyclical external volume expansion more robustly induces angiogenesis, with a lower rate of complications.[30,34,35] In animals, both preconditioning and postconditioning with external volume expansion have been shown to increase the survival of adipose grafts.[30,36] In the combined external volume expansion plus allograft adipose matrix treatment, we observed a relevant increase of volume of the grafts (41 percent) from week 4 to week 12, likely because of gradual recellularization of the acellular graft by migrating adipocytes. Instead, the rate of reabsorption observed in control adipose tissue grafts is consistent with that reported in clinical practice.[5,6,37–39]

Despite not evaluating the molecular pathways elicited by the allograft adipose matrix, our analysis is consistent with previous reports on the capacity of acellular adipose matrices to promote adipocyte migration and proliferation.[15,17,18,22] Infiltration of inflammatory cells along the external border of the scaffold might play a relevant role in adipogenic processes.[24,27,40] The allograft adipose matrix also supports endothelial proliferation, possibly because of the presence of proangiogenic factors within decellularized adipose matrices.[22,41,42] In this study, external volume expansion did not improve the survival of allograft adipose matrix plus adipose tissue grafts; this might relate to the creation by the allograft adipose matrix of an additional physical barrier to the diffusion of metabolites to grafted adipocytes (Fig. 5).[24,27]

The innovation of this allograft adipose matrix lies in its scalability for clinical use. Previous literature had investigated adipose scaffolds derived from small animals, swine, or human surgical discards: although the use of these scaffolds provided helpful experimental insights, it could not translate into large-scale clinical adoption.[2,12,13,15–22,43] Small animals offer a minimal source of tissue. Human surgical discarded tissues also provide a limited amount of fat; in addition, they present challenges related to the standardization of tissue procurement, preservation, transport, and processing. Swine could represent an ideal tissue source (high availability, controlled quality), but

research needs to confirm the lack of xenogenic immune reactions of decellularized porcine adipose tissue and the presence of biological properties comparable to those of human matrices. Instead, human cadaveric donors provide a controlled and standardized source of readily available fat, retaining the biochemical characteristics of native human tissue. In the future, genetically modified swine and tissue-engineered adipose scaffolds will provide new therapeutic opportunities in this field.

Our study has limitations. We have not assessed the mechanistic pathways elicited by the allograft adipose matrix, and have postulated that phenomena similar to those described previously for other acellular adipose matrices might occur. We also used human lipoaspirate grafts in immunodeficient animals. The lack of cellular components in the allograft adipose matrix allows its safe use as an allograft (human to human); however, some degree of rejection might be observed in immunocompetent animal models. We also chose to measure the graft cross-sectional area as a surrogate method to assess whole-graft volume retention; however, we believe our findings provide correct estimates. In addition, even if 0.3 cc represents a large-volume graft in rodents, this is a very small volume in humans: future research will need to investigate whether critical surface-to-volume ratios exist. For larger volumes, host cell infiltration may take longer; however, as the allograft adipose matrix is decellularized, there should not be concerns for necrosis at the graft core. Our analysis of the inflammatory response elicited by the grafts has been only qualitative. Finally, clinical use of external volume expansion has been hindered by poor patient compliance; however, recent innovations may reduce these challenges.[30]

CONCLUSIONS

In summary, we show that the combined use of external volume expansion and an allograft adipose matrix graft for soft-tissue reconstruction leads to a higher volume retention and better tissue preservation compared to adipose tissue grafts. The allograft adipose matrix supports tissue regeneration in the form of adipogenesis and angiogenesis. This approach might transform best practice in the reconstruction of soft-tissue defects, if outcomes are confirmed in large animals or in preliminary clinical trials. Of note, clinical safety evaluations of the allograft adipose matrix has been completed and human studies are currently ongoing.[33,44]

Giorgio Giatsidis, M.D., Ph.D.
Division of Plastic Surgery
Department of Surgery
Brigham and Women's Hospital
Harvard Medical School
75 Francis Street
Boston, Mass. 02115
ggiatsidis@bwh.harvard.edu
Instagram: drgiatsidis
Twitter: @drgiatsidis

Dennis P. Orgill, M.D., Ph.D.
Division of Plastic Surgery
Department of Surgery
Brigham and Women's Hospital
Harvard Medical School
75 Francis Street
Boston, Mass. 02115
dorgill@bwh.harvard.edu

ACKNOWLEDGMENTS

This study was funded in part from a sponsored research agreement from the Musculoskeletal Transplant Foundation and a grant from the Gillian Reny Stepping Strong Fund, both to the Brigham and Women's Hospital. The authors are grateful for the technical support and contribution provided by Benjamin Schilling, Marc Jacobs, and Anthony Haddad, M.D.

REFERENCES

1. Morrison WA, Marre D, Grinsell D, Batty A, Trost N, O'Connor AJ. Creation of a large adipose tissue construct in humans using a tissue-engineering chamber: A step forward in the clinical application of soft tissue engineering. *EBioMedicine* 2016;6:238–245.
2. Zhang Q, Johnson JA, Dunne LW, et al. Decellularized skin/adipose tissue flap matrix for engineering vascularized composite soft tissue flaps. *Acta Biomater.* 2016;35:166–184.
3. Mirzabeigi MN, Smartt JM, Nelson JA, Fosnot J, Serletti JM, Wu LC. An assessment of the risks and benefits of immediate autologous breast reconstruction in patients undergoing postmastectomy radiation therapy. *Ann Plast Surg.* 2013;71:149–155.
4. Chang NJ, Waughlock N, Kao D, Lin CH, Lin CH, Hsu CC. Efficient design of split anterolateral thigh flap in extremity reconstruction. *Plast Reconstr Surg.* 2011;128:1242–1249.
5. Suga H, Eto H, Aoi N, et al. Adipose tissue remodeling under ischemia: Death of adipocytes and activation of stem/progenitor cells. *Plast Reconstr Surg.* 2010;126:1911–1923.
6. Suga H, Matsumoto D, Inoue K, et al. Numerical measurement of viable and nonviable adipocytes and other cellular components in aspirated fat tissue. *Plast Reconstr Surg.* 2008;122:103–114.
7. Eto H, Kato H, Suga H, et al. The fate of adipocytes after nonvascularized fat grafting: Evidence of early death and replacement of adipocytes. *Plast Reconstr Surg.* 2012;129:1081–1092.
8. Kato H, Mineda K, Eto H, et al. Degeneration, regeneration, and cicatrization after fat grafting: Dynamic total tissue remodeling during the first 3 months. *Plast Reconstr Surg.* 2014;133:303e–313e.

9. Paillocher N, Florczak AS, Richard M, et al. Evaluation of mastectomy with immediate autologous latissimus dorsi breast reconstruction following neoadjuvant chemotherapy and radiation therapy: A single institution study of 111 cases of invasive breast carcinoma. *Eur J Surg Oncol.* 2016;42:949–955.
10. Macadam SA, Zhong T, Weichman K, et al. Quality of life and patient-reported outcomes in breast cancer survivors: A multicenter comparison of four abdominally based autologous reconstruction methods. *Plast Reconstr Surg.* 2016;137:758–771.
11. Daly LT, Mowlds D, Brodsky MA, Abrouk M, Gandy JR, Wirth GA. Breast microsurgery in plastic surgery literature: A 21-year analysis of publication trends. *J Reconstr Microsurg.* 2016;32:276–284.
12. Wang L, Johnson JA, Zhang Q, Beahm EK. Combining decellularized human adipose tissue extracellular matrix and adipose-derived stem cells for adipose tissue engineering. *Acta Biomater.* 2013;9:8921–8931.
13. Turner AE, Flynn LE. Design and characterization of tissue-specific extracellular matrix-derived microcarriers. *Tissue Eng Part C Methods* 2012;18:186–197.
14. Haddad SM, Omidi E, Flynn LE, Samani A. Comparative biomechanical study of using decellularized human adipose tissues for post-mastectomy and post-lumpectomy breast reconstruction. *J Mech Behav Biomed Mater.* 2016;57:235–245.
15. Flynn LE. The use of decellularized adipose tissue to provide an inductive microenvironment for the adipogenic differentiation of human adipose-derived stem cells. *Biomaterials* 2010;31:4715–4724.
16. Yu C, Bianco J, Brown C, et al. Porous decellularized adipose tissue foams for soft tissue regeneration. *Biomaterials* 2013;34:3290–3302.
17. Brown CF, Yan J, Han TT, Marecak DM, Amsden BG, Flynn LE. Effect of decellularized adipose tissue particle size and cell density on adipose-derived stem cell proliferation and adipogenic differentiation in composite methacrylated chondroitin sulphate hydrogels. *Biomed Mater.* 2015;10:045010.
18. Turner AE, Yu C, Bianco J, Watkins JF, Flynn LE. The performance of decellularized adipose tissue microcarriers as an inductive substrate for human adipose-derived stem cells. *Biomaterials* 2012;33:4490–4499.
19. Flynn L, Prestwich GD, Semple JL, Woodhouse KA. Adipose tissue engineering with naturally derived scaffolds and adipose-derived stem cells. *Biomaterials* 2007;28:3834–3842.
20. Brown BN, Freund JM, Han L, et al. Comparison of three methods for the derivation of a biologic scaffold composed of adipose tissue extracellular matrix. *Tissue Eng Part C Methods* 2011;17:411–421.
21. Giatsidis G, Dalla Venezia E, Venezia ED, De Stefani D, Rizzuto R, Bassetto F. Breast tissue engineering: Decellularized scaffolds derived from porcine mammary glands. *Plast Reconstr Surg.* 2015;136(Suppl):1391.
22. Han TT, Toutounji S, Amsden BG, Flynn LE. Adipose-derived stromal cells mediate in vivo adipogenesis, angiogenesis and inflammation in decellularized adipose tissue bioscaffolds. *Biomaterials* 2015;72:125–137.
23. Giatsidis G, Succar J, Haddad A, et al. Preclinical optimization of a shelf-ready, human-derived, decellularized allograft adipose matrix. *Tissue Eng Part A* 2019;25:271–287.
24. Lujan-Hernandez J, Lancerotto L, Nabzdyk C, et al. Induction of adipogenesis by external volume expansion. *Plast Reconstr Surg.* 2016;137:122–131.
25. Kao HK, Hsu HH, Chuang WY, et al. External volume expansion modulates vascular growth and functional maturation in a swine model. *Sci Rep.* 2016;6:25865.
26. Reddy R, Iyer S, Sharma M, et al. Effect of external volume expansion on the survival of fat grafts. *Indian J Plast Surg.* 2016;49:151–158.
27. Giatsidis G, Cheng L, Facchin F, et al. Moderate-intensity intermittent external volume expansion optimizes the soft-tissue response in a murine model. *Plast Reconstr Surg.* 2017;139:882–890.
28. Heit YI, Lancerotto L, Mesteri I, et al. External volume expansion increases subcutaneous thickness, cell proliferation, and vascular remodeling in a murine model. *Plast Reconstr Surg.* 2012;130:541–547.
29. Khouri RK, Rigotti G, Cardoso E, Khouri RK, Biggs TM. Megavolume autologous fat transfer: Part II. Practice and techniques. *Plast Reconstr Surg.* 2014;133:1369–1377.
30. Giatsidis G, Cheng L, Haddad A, et al. Noninvasive induction of angiogenesis in tissues by external suction: Sequential optimization for use in reconstructive surgery. *Angiogenesis* 2018;21:61–78.
31. Ye Y, Liao Y, Lu F, Gao J. Daily suction provided by external volume expansion inducing regeneration of grafted fat in a murine model. *Plast Reconstr Surg.* 2017;139:392e–402e.
32. Coleman SR. Structural fat grafting. *Aesthet Surg J.* 1998;18:386, 388.
33. Musculoskeletal Transplant Foundation. Allograft adipose matrix (AAM) in subcutaneous dorsal wrist. Available at: https://clinicaltrials.gov/ct2/show/NCT02445118?term=adipose+%2C+allograft&rank=1. Accessed August 31, 2018.
34. Wei S, Orgill DP, Giatsidis G. Delivery of External Volume Expansion (EVE) through Micro-deformational Interfaces Safely Induces Angiogenesis in a Murine Model of Intact Diabetic Skin with Endothelial Cell Dysfunction (ECD). *Plast Reconstr Surg.*
35. Rhodius P, Haddad A, Matsumine H, et al. Non-invasive flap preconditioning by foam-mediated external suction improves the survival of fasciocutaneous axial-pattern flaps in a type 2 diabetic murine model. *Plast Reconstr Surg.* 2018;142:872e–883e.
36. Wei S, Liu W, Gundogan B, Moscoso AV, Orgill DP, Giatsidis G. Delayed post-conditioning with external volume expansion improves survival of adipose tissue grafts in a murine model. *Plast Reconstr Surg.* 2019;143:99e–110e.
37. Mashiko T, Yoshimura K. How does fat survive and remodel after grafting? *Clin Plast Surg.* 2015;42:181–190.
38. Rao A, Saadeh PB. Defining fat necrosis in plastic surgery. *Plast Reconstr Surg.* 2014;134:1202–1212.
39. Khouri RK Jr, Khouri RE, Lujan-Hernandez JR, Khouri KR, Lancerotto L, Orgill DP. Diffusion and perfusion: The keys to fat grafting. *Plast Reconstr Surg Glob Open* 2014;2:e220.
40. Zampell JC, Aschen S, Weitman ES, et al. Regulation of adipogenesis by lymphatic fluid stasis: Part I. Adipogenesis, fibrosis, and inflammation. *Plast Reconstr Surg.* 2012;129:825–834.
41. Kosaraju R, Rennert RC, Maan ZN, et al. Adipose-derived stem cell-seeded hydrogels increase endogenous progenitor cell recruitment and neovascularization in wounds. *Tissue Eng Part A* 2016;22:295–305.
42. Frueh FS, Später T, Lindenblatt N, et al. Adipose tissue-derived microvascular fragments improve vascularization, lymphangiogenesis, and integration of dermal skin substitutes. *J Invest Dermatol.* 2017;137:217–227.
43. Kim JS, Choi JS, Cho YW. Cell-free hydrogel system based on a tissue-specific extracellular matrix for in situ adipose tissue regeneration. *ACS Appl Mater Interfaces.* 2017;9(:8581–8588.
44. Musculoskeletal Transplant Foundation. In-vivo assessment of adipose allograft extracellular matrix in abdominoplasty patients. Available at: https://clinicaltrials.gov/ct2/show/NCT02845180?term=adipose+%2C+allograft&rank=2. Accessed August 31, 2018.